

## State, trait and biochemical influences on human anterior cingulate function

Murat Yücel,<sup>a,b,c,\*</sup> Ben J. Harrison,<sup>a,c</sup> Stephen J. Wood,<sup>a,c,e</sup> Alex Fornito,<sup>a,d</sup> Kerrie Clarke,<sup>a</sup> R. Mark Wellard,<sup>e,f</sup> Sue Cotton<sup>b</sup> and Christos Pantelis<sup>a,c</sup>

<sup>a</sup>Melbourne Neuropsychiatry Centre, Australia

<sup>b</sup>ORYGEN Research Centre, Melbourne, Australia

<sup>c</sup>Department of Psychiatry, The University of Melbourne, Australia

<sup>d</sup>Department of Psychology, The University of Melbourne, Australia

<sup>e</sup>Brain Research Institute, Austin and Repatriation Medical Centre, Melbourne, Australia

<sup>f</sup>Queensland University of Technology, Brisbane, QLD, Australia

Received 12 July 2006; revised 17 August 2006; accepted 24 August 2006  
Available online 26 December 2006

The dorsal part of the human anterior cingulate cortex (dACC) is reliably activated in situations requiring cognitive control, especially during states of conflict. However, little is known about how individual differences in the neural characteristics of the dACC and major dimensions of behavior, affect this brain response. We recruited 28 healthy adults and employed a multi-modal neuroimaging approach combined with a task designed to specifically activate the human dACC and statistical path analysis to demonstrate clear roles for intelligence, personality and concentrations of neuronal *N*-acetylaspartate in determining dACC activation. These influences were comparable in magnitude to those associated with the experience of conflict. Our findings extend current understandings of the neural substrates of cognitive control by modeling the effect of neuronal viability, intelligence, and personality, on dACC activation. They also highlight the importance of considering enduring personal characteristics when mapping human brain–behavior relationships.

© 2006 Elsevier Inc. All rights reserved.

**Keywords:** Cingulate; Conflict; fMRI; MRS; Intelligence; Personality; Motivation

Two decades of functional neuroimaging research have demonstrated that the dorsal anterior cingulate cortex (dACC), situated on the medial surface of the frontal lobes, is involved in a broad range of human behavior, including cognitive control, reward-based learning, pain, emotion, autonomic and motor function (Bush et al., 2000; Paus, 2001; Picard and Strick, 2001;

Bush et al., 2002; Critchley et al., 2003; Vogt, 2005). There is now also extensive evidence linking dACC dysfunction to a number of psychiatric disorders (Benes et al., 1993; Yücel et al., 2003; Critchley et al., 2003; Ridderinkhof et al., 2004), as well as normal and abnormal personality traits (Pujol et al., 2002; Canli et al., 2004; Kumari et al., 2004; Gray et al., 2005; Whittle et al., 2006), suggesting it is a vulnerable part of an important and common pathway involved in the regulation of behavior, cognition and emotion. Recently, particular interest has been paid to understanding dACC activation in response to states of conflict (Kerns et al., 2004; Matsumoto and Tanaka, 2004; Brown and Braver, 2005). According to one prominent theory, this neuronal response may reflect a *conflict monitoring* role for the dACC (Botvinick et al., 2001, 2004), whereby this region supports goal-directed behavior by specifically reacting to, or predicting, the occurrence of conflicts in performance (e.g. response errors), in turn, signaling the need for greater cognitive control.

To date, most research examining dACC activation in conflict paradigms has focused on transient, state-related changes in activation by manipulating the nature and degree of conflict within a given task (Botvinick et al., 2001, 2004; Garavan et al., 2003; Brown and Braver, 2005). However, it is not yet clear just how influential state-related factors are in determining dACC activation with respect to other major influences on human behavior and brain function, such as individual differences in the underlying neurobiology of the dACC and/or overarching trait characteristics of the person, such as intelligence and personality (Grachev et al., 2001; Gray et al., 2003, 2005).

Previous research in healthy populations has demonstrated that individuals with higher intelligence typically show superior behavioral performance (e.g. they make fewer errors) on challenging cognitive tasks, including response-conflict paradigms (Jung et al., 2000; Gray et al., 2003). On the basis of the conflict monitoring account, one would predict that such individuals with

\* Corresponding author. Melbourne Neuropsychiatry Centre, c/o AG Building (Level 3), 161 Barry Street, Carlton South, Victoria 3053, Australia. Fax: +613 8345 0599.

E-mail address: murat@unimelb.edu.au (M. Yücel).

Available online on ScienceDirect (www.sciencedirect.com).



reliable single-subject level activations. This is important for the current study as it facilitates our aim of correlating functional activation patterns with individual differences in personality, intelligence and brain metabolites in order to better understand the nature of the relationships between these measures. In our version of the MSIT, the numbers 0–3 were presented in strings of three, with one always being different to the other two (Fig. 2). Subjects were instructed to indicate the identity (not the position) of the number that was different from the other two items by pressing the appropriate button on a response box placed on their stomach, i.e., **1** **2** **3**. Responses were made with one of three fingers; the index finger to indicate 1, the middle finger to indicate 2, and the ring finger to indicate 3. During congruent (C) task trials the number always matched the position on the response box and was flanked by the number 0. During incongruent (I) task trials numbers never matched the response position and were flanked by incongruent numbers. Subjects were informed that scans would begin and end with fixation (fixation trials=F) for 60 s, between which they would see eight alternating block pairs of C and I trials (i.e. 16 blocks), lasting 30 s per block, were presented (i.e. FCICICIFCICICIF). Stimulus and inter-stimulus intervals were 2000 ms and 500 ms, respectively. For all trials, subjects were instructed to answer as quickly and accurately as possible. Prior to scanning, all participants completed a practice run of the task consisting of one block of 12 C and one block of 12 I trials.

Subjects completed a practice of the task (24 trials, presented as two blocks of 12 C trials and 12 I trials) pre-scanning. During the scanning trials, behavioral reaction time (RT) and percentage error scores were recorded via a notebook computer. Interference effects (MSIT-rt) were calculated by subtracting the mean RT for the C trials across all blocks from the mean RT of the I trials across all blocks. Response errors were calculated by summing all commission (e.g. responding '1' when the correct answer was '2') and omission errors (missed responses) across the C and I trials, although the greatest percentage of errors occurred during the latter trials. Data were analyzed with a two-way, within-groups repeated measures analysis of variance (ANOVA) in Statistical Package for the Social Sciences (SPSS) version 11.0 after checking for data normality. Path analysis, a multivariate statistical technique that enables examination of the nature of interactions amongst measures with shared variance, was performed using AMOS (Analysis of Moment Structures) (Arbuckle, 1999). All data were screened for normality prior to entry into a path analysis. The MSIT-err variable was log-transformed to ensure normality of

distribution (Tabachnick and Fidell, 2001). A post-hoc comparison of the paths associated with the trait and state variables was conducted using the Chi-squared difference procedure detailed in Kline (2005).

#### Imaging acquisition and analysis

All individual MRI sequences were acquired in a single scanning session using a 3T GE Signa Horizon LX human scanner (General Electric, Milwaukee, WI, USA). Prior to scanning, subjects were introduced to a 'mock scanner' in order to familiarise them with the MRI environment. Following the mock session, subjects were taken to the actual scanner and had their head fixed on the table using a Velcro® strap over the forehead. Scanning sequences consisted of a scout localiser, fMRI, T1-weighted anatomical sequence and MRS, in that order. Data were transferred to a Linux 2.4.27 workstation (Debian Sarge) for image pre-processing and analysis.

Functional MRI (fMRI) data were acquired as a series of single shot gradient-recalled echo-echo planar imaging (GRE-EPI) volumes providing T2\*-weighted BOLD contrast. The image acquisition parameters for the functional scans were TR/TE/flip-angle, 3000 ms/40 ms/60°, FOV of 24 centimetres (cm) producing a voxel size of 1.875 × 1.875 × 4.0 mm and 25 slices for full-brain coverage. The first four images in each run were automatically discarded to allow the magnetization to reach a steady-state equilibrium. Each 30 s block in the experiment had 10 volumes resulting in 80 volumes in total for the C condition and 80 volumes in total for the I condition.

Analysis of the fMRI data was carried out using FEAT (fMRI Expert Analysis Tool) Version 5.4, part of FSL (FMRIB's Software Library, [www.fmrib.ox.ac.uk/fsl](http://www.fmrib.ox.ac.uk/fsl)). The following pre-statistics processing was applied; motion correction using MCFLIRT (Jenkinson et al., 2002); non-brain removal using BET (Smith, 2002); spatial smoothing using a Gaussian kernel of FWHM 5 mm; mean-based intensity normalisation of all volumes by the same factor; high-pass temporal filtering (Gaussian-weighted LSF straight line fitting, with sigma=30.0 s). Time-series statistical analysis was carried out using FILM with local autocorrelation correction (Woolrich et al., 2001). Individual subject Z (Gaussian transformed) statistical images were thresholded using clusters determined by  $Z > 2.7$  and a whole-brain (corrected) cluster significance threshold of  $P = 0.05$  (Worsley et al., 1992). Twenty-five of the twenty-eight subjects showed suprathreshold dACC activity; two additional subjects showed activity at a lowered

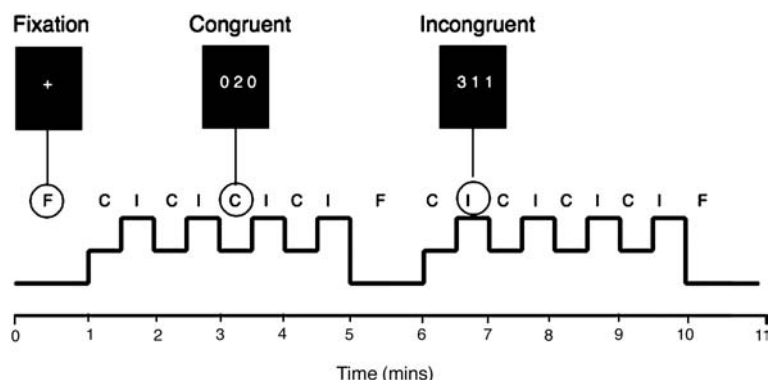


Fig. 2. Example of the trials and block design of the MSIT paradigm.

Z-score of 2.33 (whole-brain cluster-wise corrected); one subject showed subthreshold activity. For each individual, we extracted a converted percentage signal change value ( $I>C$ ) of the BOLD response from the dACC cluster maxima using Featquery in FSL. We used the peak voxel signal for each individual in preference to summing activity over a larger area in a standard space (e.g. an area around the peak voxel or the MRS volume of interest) to minimise averaging over non-significant voxels. In previous work, we have found this individually tailored voxel is representative of the overall activated cluster and provides a more reliable association with the behavioral indices of MSIT performance (unpublished data). Additional, group-level analysis was carried out using FLAME (FMRIB's Local Analysis of Mixed Effects) (Beckmann et al., 2003; Woolrich et al., 2004). Z (Gaussian transformed) statistic images were thresholded using clusters determined by  $Z>4.0$  and a whole-brain (corrected) cluster significance threshold of  $P<0.05$  (Worsley et al., 1992). Registration to high resolution and standard space images was carried out using FLIRT (Jenkinson and Smith, 2001; Jenkinson et al., 2002).

Volume localized proton magnetic resonance spectroscopy ( $^1\text{H}$ -MRS) was recorded using a short-echo point resolved spectroscopy sequence (PRESS; TR=3000 ms, TE=30 ms, NEX=128; with a nominal voxel size  $\sim 6.5\text{ cm}^3$ ) from the dACC bilaterally. MRS voxels were placed in each hemisphere, separated by the medial wall boundary of the frontal lobes that were designed to encompass the dACC. The posterior boundary of the voxel was  $\sim 10$  mm posterior of a vertical line from the anterior commissure (AC) orthogonal to the AC–PC (posterior commissure) line. The inferior border was  $\sim 5$  mm superior to the top edge of the corpus callosum while the medial border was 1–2 slices lateral to the parasagittal slice on the T1 structural image for each hemisphere. For volume-localized spectra, absolute levels of *N*-acetyl compounds (NAA+NAAg), creatine plus phosphocreatine (Cr) and choline-containing compounds (Cho) were measured. Metabolite concentrations were determined for each ROI (corrected for estimated tissue content) with LCModel software (Provencher, 1993). This software used a library of reference spectra in a basis set recorded specifically for the scanner and calibrated using the tissue water signal as an internal standard. The LCModel fitting algorithm uses the multiple peaks

contributing to an individual metabolite spectrum to estimate the tissue content of each metabolite (Provencher, 1993). The residual signal corresponds to, and is fitted by, additional broad peaks representing unknown metabolites and other factors such as macromolecular components with short T2 relaxation times. As the left and right values for each metabolite were highly correlated ( $R=0.46$ – $0.88$ ;  $P<0.01$ ), we collapsed these values. The chosen MRS parameters provided robust signals with a FWHM of 0.06 and a signal-to-noise ratio of 15.90. The output from LCModel also includes the Cramer–Rao lower bounds (CRLB), which is a measure of reliability. The mean CRLB for NAA was 5.3. A sample spectra from the dACC region of interest is shown in Fig. 3.

## Results

### Performance and functional analyses

As in previous studies, we found that MSIT performance produced a large and significant response conflict effect as indexed by significantly longer reaction time (RT) in the incongruent compared to congruent condition (RT difference between conditions; MSIT-rt;  $M=331$  ms;  $F=509.5$ ;  $P<0.0001$ ). In addition, the MSIT generated significant error-related response conflicts, as reflected by significantly greater response errors (commission and omission) in the incongruent compared to congruent condition ( $F=16.13$ ;  $P<0.0001$ ). The overall percentage of errors committed (MSIT-err) during performance was 2.7%. Importantly, the task produced significant and robust supra-threshold activation of the dACC in 25 of our 28 individual subjects ( $Z>2.70$ ;  $P<0.05$  whole-brain, cluster-wise corrected). The foci of maximal activation in the group-defined cluster was very similar to that of previous studies (Bush et al., 2003; Heckers et al., 2004), supporting the robustness of this task as a probe of dACC function. For each individual subject, we extracted a maximum percentage signal change value (dACC peak activation) from their activated cluster using Featquery in FSL (<http://www.fmrib.ox.ac.uk/fsl/feat5/featquery.html>) and this served as the primary dependent variable (DV) for the path analysis.

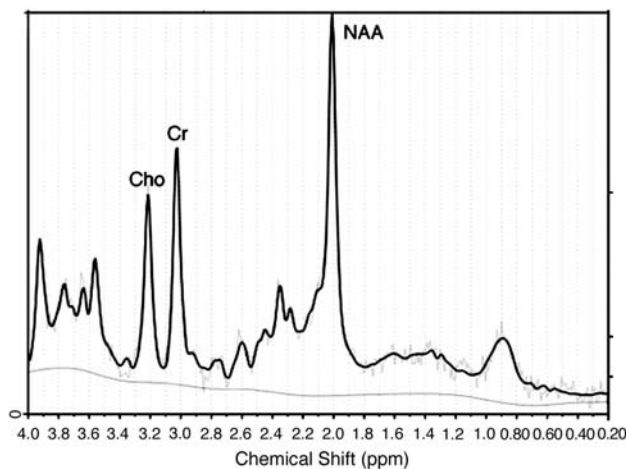


Fig. 3. Sample MRS spectra from the dACC region highlighting the three main metabolite peaks; *N*-acetyl compounds (NAA), creatine plus phosphocreatine (Cr) and choline-containing compounds (Cho).

### Path analysis

In total, five independent variables (IVs) were included in subsequent multivariate analyses. The breakdown of these IVs was classified as (i) trait (IQ, BAS); (ii) biochemical (NAA) and (iii) behavioral state measures of response conflict (MSIT-rt, MSIT-err). Indices of intelligence (IQ) and sensitivity to reward (BAS) were derived using measures similar to those used in previous studies (Wechsler, 1999; Torrubia et al., 2001). Measures of NAA concentration within the dACC were obtained using proton MRS from a predicted MSIT-dACC region of activation (Bush et al., 2003; Heckers et al., 2004) (Fig. 4). Refer to Table 1a for descriptive statistics of these variables.

Path analysis was performed using AMOS (Analysis of Moment Structures) (Arbuckle, 1999). The correlation matrix of Pearson's Product Moment Correlation Coefficients was first examined to determine linearity and the degree of relationship between the variables of interest. All variables included in the analyses correlated moderately ( $R \geq 0.3$ ;  $R^2 \geq 0.09$ ) (Cohen, 1988) with at least one other variable of interest (Table 1a), supporting the inclusion of each variable to the path analysis model. Variables that showed strong correlations with dACC activation were MSIT-rt, MSIT-err, and the BAS scores.

The initial over-fitted path model was modified in a stepwise fashion (i.e. removing and adding variables path-by-path), on the basis of the aforementioned literature, and the significance of the Critical Ratio indices for each path as a guide. Model stability was retested after each path modification. This procedure was iterated several times before yielding the final and 'best' path model (Fig. 5a). This model explained 67% of the variance in dACC activation. The test of absolute fit of the final model indicated that the model was a good fit to the data ( $\chi^2 = 5.03$ ;  $P = 0.83$ ). Further, support for the fit of the model was derived from the relative fit indices (Tucker–Lewis Index (TLI) = 1.019; Root Mean Square Error of Approximation (RMSEA)  $\leq 0.0001$ ). Combined, these indices indicate that the model was parsimonious. The Critical Ratio indices for each of the path associations in the final model can be seen in Table 1b while the nature and strength of the direct and indirect influences on dACC activation can be seen in Table 1c.

The strongest direct influence on dACC activation was MSIT-err (Table 1b; Fig. 5a). These findings are consistent with a bottom-up model of conflict monitoring (Botvinick et al., 2001, 2004), and suggest that state-related task demands are indeed an important driving influence on dACC activation. However, our results also illustrate the importance of individual trait characteristics. As predicted, IQ had *both* direct and indirect influences on dACC activation. In the direct path, IQ was *positively* associated with dACC activation, while in the indirect path it was *negatively* associated with behavioral performance. In contrast, reward sensitivity (or BAS) only exerted a direct influence on dACC activation. Consistent with previous research, the effect of reward sensitivity was independent of IQ and behavioral performance (Gray and Braver, 2002; Gray et al., 2005). Importantly, there was no significant difference between the contributions of trait-related measures (BAS and IQ) and state-related measures (MSIT-err and MSIT-rt) to dACC activity ( $\chi^2 = 7.16$ ;  $P > 0.05$ ). This indicates that state and trait characteristics are equally important determinants of dACC activation. Further, NAA only exerted an indirect effect on dACC activation through IQ, and was not directly predictive of conflict-related dACC activation.

Exploratory analyses incorporating the other two main neurochemical measures derived from the spectroscopy data (Cho and Cr) revealed that both metabolites were significant predictors of dACC activation, albeit indirectly, through task performance measures (particularly through MSIT-err). Further, age was also a significant but indirect predictor of dACC activity through Cho and NAA. However, these measures in combination only explained an additional 5% of variance in dACC activation when compared to the model with only NAA, IQ, and personality (72% versus 67%, respectively). As such, these were deemed to exert relatively minor influences on dACC activation and were not included in the final model.

### Discussion

While the dorsal part of the human anterior cingulate cortex (dACC) is reliably activated in situations of conflict, very little is known about how individual differences in the neural characteristics of the dACC and major dimensions of behavior, affect this

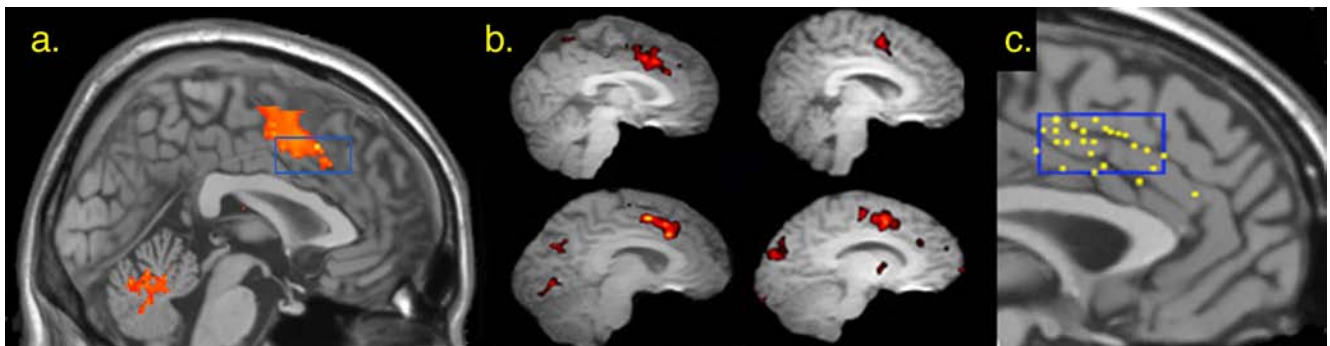


Fig. 4. Group and single-subject level dACC activation and volume localised proton MRS voxel given in sagittal orientation. (a) Illustration of the group activated cluster (group maxima in yellow [ $Z = 7.27$ ,  $P < 3.15 \times 10^{-35}$ ] with  $x, y, z$  coordinates of 0, 18, 44) and the MRS voxel dimensions displayed on a canonical structural MR image (MNI, Montreal Neurological Institute, Talairach brain). (b) Representative single-subject data for four subjects showing focal activations of the dACC mapped onto subject's own structural MR image in native anatomical space. (c) Close-up of representation illustrating that single-subject activation peaks (yellow) were closely bound to the area sampled by the MRS voxel. These peak activation co-ordinates are mapped in the  $y$  and  $z$  planes on a canonical structural MR image (MNI-Talairach brain) using a representative sagittal ( $x$ -plane) slice.

Table 1  
Descriptive data and analyses

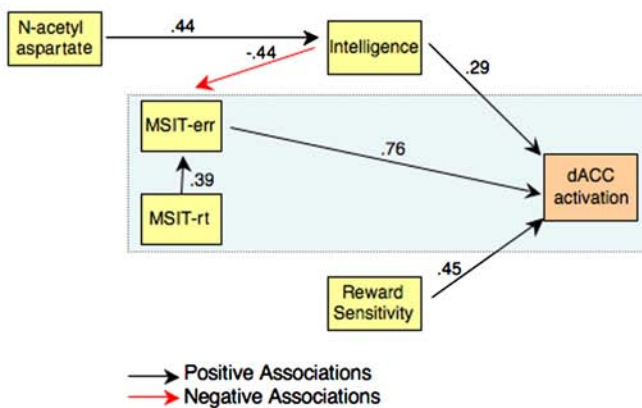
| n = 28   | dACC     | MSIT-rt  | MSIT-err   | NAA    | BAS     | IQ | Mean   | s.d.  | Range     |
|--|----------|----------|------------|--------|---------|----|--------|-------|-----------|
| <i>a: Means, standard deviations and correlation among the variables</i>   |          |          |            |        |         |    |        |       |           |
| dACC   | 1        |          |            |        |         |    | 1.46   | 0.77  | 0.38–3.34 |
| MSIT-rt  | 0.462    | 1        |            |        |         |    | 331.45 | 77.70 | 207–549   |
| MSIT-err   | 0.721    | 0.482    | 1          |        |         |    | 2.66   | 2.99  | 0–13.02   |
| NAA  | -0.110   | 0.111    | -0.190     | 1      |         |    | 8.27   | 0.63  | 7.29–9.45 |
| BAS  | 0.463    | 0.074    | 0.082      | 0.321  | 1       |    | 6.84   | 3.45  | 1–15      |
| IQ   | -0.009   | -0.119   | -0.323     | 0.440  | 0.248   | 1  | 113.00 | 11.12 | 89–130    |
| <i>b: Regression weights and critical ratios for the principal relationships between variables</i>   |          |          |            |        |         |    |        |       |           |
| Path associations  |          | Estimate | S.E.       | C.R.   | P-value |    |        |       |           |
| IQ   | NAA      | 7.801    | 3.068      | 2.543  | 0.011   |    |        |       |           |
| MSIT-err   | IQ       | -0.011   | 0.004      | -2.816 | 0.005   |    |        |       |           |
| MSIT-err   | MSIT-rt  | 0.001    | 0.001      | 2.509  | 0.012   |    |        |       |           |
| dACC   | IQ       | 0.020    | 0.009      | 2.324  | 0.020   |    |        |       |           |
| dACC   | BAS      | 0.099    | 0.025      | 3.974  | <0.001  |    |        |       |           |
| dACC   | MSIT-err | 2.046    | 0.340      | 6.010  | <0.001  |    |        |       |           |
| <i>c: Direct and indirect standardized regression weights for the relationships between the variables of interest and dACC BOLD activity</i> |          |          |            |        |         |    |        |       |           |
| Variable   |          | β-direct | β-indirect |        |         |    |        |       |           |
| MSIT-err   |          | 0.756    | 0          |        |         |    |        |       |           |
| BAS  |          | 0.454    | 0          |        |         |    |        |       |           |
| IQ   |          | 0.292    | -0.332     |        |         |    |        |       |           |
| MSIT-rt  |          | 0        | 0.295      |        |         |    |        |       |           |
| NAA  |          | 0        | -0.017     |        |         |    |        |       |           |

brain response. In the current study, we recruited 28 healthy adults and employed a multi-modal neuroimaging approach combined with statistical path analysis to demonstrate and quantify the relative influences of intelligence, personality, concentrations of neuronal N-acetylaspartate and response conflict in determining dACC activation.

A conceptual model of the current findings is shown in Fig. 5b depicting the three primary paths of influence on dACC activation. Complementing existing evidence, Path a characterizes well-known behavioral task effects and suggests that response error in particular was the primary state determinant of dACC activation.

This association between response errors and dACC activation has been previously described and is one of the founding principles of the conflict monitoring theory (Botvinick et al., 2004; Brown and Braver, 2005). Our findings suggest that the commonly observed brain-behavior association between RT-conflict and dACC activation is driven by a common association of both measures with response errors (i.e. Path a in Fig. 5). This is consistent with the view that performance errors have a specific phenomenological relevance to the activation and function of the human dACC (Brown and Braver, 2005). It may be that dACC activation to conflict reflects a ‘learned’ role for this brain region that is

**a. 'BEST FIT' FINAL MODEL**



**b. 'CONCEPTUAL' MODEL**

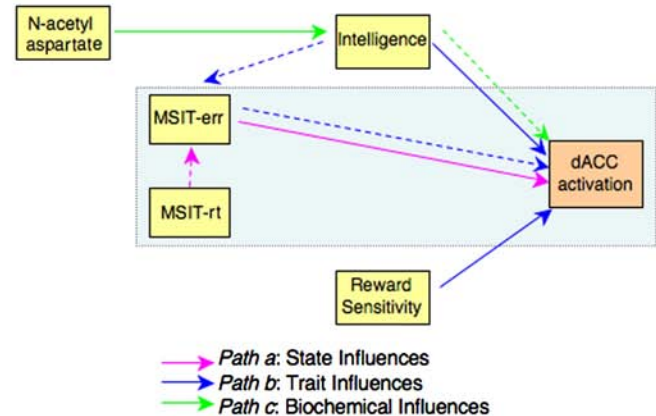


Fig. 5. Pathways of influence on dACC activation. (a) Initial model was derived from evidence in the existing empirical literature and ‘over-fitted’ to generate the best-fit model. (b) A conceptual model is also presented that highlights the pathways of influence of state, trait and biochemical factors (dashed lines represent indirect effect). The aqua box highlights the relationships typically explored in functional neuroimaging studies.

associated with predicting errors *en route* (Ridderinkhof et al., 2004; Brown and Braver, 2005). Investigations of the time-course of state-related conflict events and dACC activation will be better suited to confirming such relationships.

In addition to the state influences described in *Path a*, *Path b* suggests that individual differences in enduring trait phenomena also play an equally important role in determining dACC activation. Supporting our original assertion, we found that IQ has a direct modulatory role over dACC activation in response to conflict, in addition to an indirect effect that was mediated by response errors. The indirect negative influence of IQ over dACC activation indicates that, individuals with higher IQ showed better behavioral performance (as reflected by lower MSIT-err) with a concomitant decrease in dACC activation. By comparison, the direct positive influence of IQ over dACC activation may reflect differences in the neural mechanisms (i.e. differences in neural efficiency) associated with higher intelligence, of which dACC activation is a major component (Gray et al., 2003). Alternatively, increased dACC activation in individuals with higher intelligence may result from enhanced monitoring of error-likelihood that enabled subjects to better predict their probability of making errors and the need to adjust performance through increased cognitive control (Gray et al., 2003).

*Path b* is also consistent with the observations of Gray and colleagues (Gray and Braver, 2002; Gray et al., 2005) who have reported a unique direct influence of reward sensitivity on dACC activation during cognitive control paradigms, an effect that was similarly independent of IQ and task performance. However, whereas Gray and Braver (2002) and Gray et al. (2005) report higher reward sensitivity to be predictive of less dACC activation, we found a significant positive association between these two variables. One speculative interpretation of our findings is that individuals who are more sensitive to rewards are more likely to monitor for the likelihood of performance errors than those who are not reward sensitive. Alternatively, it is possible that these reward sensitive individuals were also highly anxious (high BIS) and held more negative expectations about the consequences of performance errors. This might also lead to a greater monitoring for the likelihood of performance errors. While these discrepancies clearly need further study, both findings highlight the relevance of this enduring personality trait to dACC function.

Finally, *Path c* suggests that NAA concentration, a marker of dACC neuronal integrity, has an indirect role on conflict-related activation that is mediated by its association with IQ. This contrasts with a recent study by Grachev et al. (2001), which reported a direct correlation between response conflict (i.e. RT-interference) and NAA concentration in the dACC. In our study, increased NAA was associated with increased IQ, which was in turn related to performance errors. This suggests that regional NAA concentration only has an indirect effect on response conflict and dACC activation by virtue of its overall relationship with IQ. These results are consistent with previous work showing that reduced NAA concentration is associated with a general decline of cognitive function in both clinical and healthy populations (Jung et al., 1999, 2005).

While our approach of using path analysis is useful for exploring the complicated nature of relationship among several inter-related variables, it also comes with several limitations. For example, while similar size samples have previously been used in path analysis of brain imaging data (Bullmore et al., 2000;

Seminowicz et al., 2004), typically this statistical technique requires larger samples than that of the current study. Further, while we were guided by the literature, the final model was derived in an iterative manner. As such, the current findings and their interpretation are provisional and require replication. Nonetheless, the approach allowed us to more accurately characterize the complex relationships (and shared variances) that exist between several inter-related variables than would simple pairwise correlations, facilitating interpretation of the brain imaging data in the context of individual differences in major dimensions of human behavior. We therefore expect these initial findings to form the basis of a theoretical model that can be directly tested in the future.

In conclusion, our findings extend current understandings of the neural substrates of cognitive control by modeling the effect of neuronal viability, intelligence, and personality, on dACC activation. Our findings indicate that these major dimensions of human individual differences are equally influential in predicting dACC activation as transient, conflict-related phenomena. As such, this work highlights the importance of considering these enduring personal characteristics when mapping human brain-behavior relationships. The model presented in the current study provides an initial framework for examining dACC function in healthy and clinical populations.

#### Acknowledgments

This research was supported by the National Health and Medical Research Council (NHMRC) of Australia (I.D. 236175) and the Ian Potter Foundation. Dr Murat Yücel is supported by an NHMRC Program Grant (ID: 350241). Dr. Harrison is supported by a NHMRC Training Award (I.D. 400420). Neuroimaging analysis was facilitated by the Neuropsychiatry Imaging Laboratory managed by Ms. Bridget Soulsby at the Melbourne Neuropsychiatry Centre and supported by Neurosciences Victoria. Melbourne Neuropsychiatry Centre is supported by the Department of Psychiatry, University of Melbourne and Melbourne Health. The authors would also like to thank The Mental Health Research Institute for its research and administrative support.

#### References

- Arbuckle, J.L., 1999. AMOS Graph version 4.01. SmallWaters Corporation, Chicago, IL.
- Beckmann, C.F., Jenkinson, M., Smith, S.M., 2003. General multilevel linear modeling for group analysis in fMRI. *Neuroimage* 20, 1052–1063.
- Benes, F.M., 1993. Relationship of cingulate cortex to schizophrenia and other psychiatric disorders. In: Vogt, B.A., Gabriel, M.S. (Eds.), *Neurobiology of Cingulate Cortex and Limbic Thalamus: A Comprehensive Handbook*. Birkhauser, Boston, pp. 580–605.
- Botvinick, M.M., Braver, T.S., Barch, D.M., Carter, C.S., Cohen, J.D., 2001. Conflict monitoring and cognitive control. *Psychol. Rev.* 108, 624–652.
- Botvinick, M.M., Cohen, J.D., Carter, C.S., 2004. Conflict monitoring and anterior cingulate cortex: an update. *Trends Cogn. Sci.* 8, 539–546.
- Brown, J.W., Braver, T.S., 2005. Learned predictions of error likelihood in the anterior cingulate cortex. *Science* 307, 1118–1121.
- Bullmore, E., Horwitz, B., Honey, G., Brammer, M., Williams, S., Sharma, T., 2000. How good is good enough in path analysis of fMRI data? *NeuroImage* 11, 289–301.
- Bush, G., Luu, P., Posner, M.I., 2000. Cognitive and emotional influences in anterior cingulate cortex. *Trends Cogn. Sci.* 4, 215–222.

- Bush, G., Vogt, B.A., Holmes, J., Dale, A.M., Greve, D., Jenike, M.A., Rosen, B.R., 2002. Dorsal anterior cingulate cortex: a role in reward-based decision making. *Proc. Natl. Acad. Sci. U. S. A.* 99, 523–528.
- Bush, G., Shin, L.M., Holmes, J., Rosen, B.R., Vogt, B.A., 2003. The Multi-Source Interference Task: validation study with fMRI in individual subjects. *Mol. Psychiatry* 8, 60–70.
- Canli, T., Amin, Z., Haas, B., Omura, K., Constable, R.T., 2004. A double dissociation between mood states and personality traits in the anterior cingulate. *Behav. Neurosci.* 118, 897–904.
- Cohen, J., 1988. *Statistical Power Analysis for the Behavioral Sciences*, 2nd ed. Lawrence Erlbaum Associates, Hillsdale, NJ.
- Critchley, H.D., Mathias, C.J., Josephs, O., O'Doherty, J., Zanini, S., Dewar, B.K., Cipolotti, L., Shallice, T., Dolan, R.J., 2003. Human cingulate cortex and autonomic control: converging neuroimaging and clinical evidence. *Brain* 126, 2139–2152.
- Garavan, H., Ross, T.J., Kaufman, J., Stein, E.A., 2003. A midline dissociation between error-processing and response-conflict monitoring. *NeuroImage* 20, 1132–1139.
- Grachev, I.D., Kumar, R., Ramachandran, T.S., Szevenyeni, N.M., 2001. Cognitive interference is associated with neuronal marker *N*-acetyl aspartate in the anterior cingulate cortex: an in vivo (1)H-MRS study of the Stroop Color–Word task. *Mol. Psychiatry* 6, 496, 529–439.
- Gray, J.R., Braver, T.S., 2002. Personality predicts working-memory-related activation in the caudal anterior cingulate cortex. *Cogn. Affect. Behav. Neurosci.* 2, 64–75.
- Gray, J.R., Chabris, C.F., Braver, T.S., 2003. Neural mechanisms of general fluid intelligence. *Nat. Neurosci.* 6, 316–322.
- Gray, J.R., Burgess, G.C., Schaefer, A., Yarkoni, T., Larsen, R.J., Braver, T.S., 2005. Affective personality differences in neural processing efficiency confirmed using fMRI. *Cogn. Affect. Behav. Neurosci.* 5, 182–190.
- Heckers, S., Weiss, A.P., Deckersbach, T., Goff, D.C., Morecraft, R.J., Bush, G., 2004. Anterior cingulate cortex activation during cognitive interference in schizophrenia. *Am. J. Psychiatry* 161, 707–715.
- Jenkinson, M., Smith, S., 2001. A global optimisation method for robust affine registration of brain images. *Med. Image Anal.* 5, 143–156.
- Jenkinson, M., Bannister, P., Brady, M., Smith, S., 2002. Improved optimization for the robust and accurate linear registration and motion correction of brain images. *NeuroImage* 17, 825–841.
- Jung, R.E., Yeo, R.A., Chiulli, S.J., Sibbitt Jr., W.L., Weers, D.C., Hart, B.L., Brooks, W.M., 1999. Biochemical markers of cognition: a proton MR spectroscopy study of normal human brain. *NeuroReport* 10, 3327–3331.
- Jung, R.E., Yeo, R.A., Chiulli, S.J., Sibbitt Jr., W.L., Brooks, W.M., 2000. Myths of neuropsychology: intelligence, neurometabolism, and cognitive ability. *Clin. Neuropsychol.* 14, 535–545.
- Jung, R.E., Haier, R.J., Yeo, R.A., Rowland, L.M., Petropoulos, H., Levine, A.S., Sibbitt, W.L., Brooks, W.M., 2005. Sex differences in *N*-acetyl-aspartate correlates of general intelligence: an 1H-MRS study of normal human brain. *NeuroImage* 26, 965–972.
- Kerns, J.G., Cohen, J.D., MacDonald III, A.W., Cho, R.Y., Stenger, V.A., Carter, C.S., 2004. Anterior cingulate conflict monitoring and adjustments in control. *Science* 303, 1023–1026.
- Kline, R.B., 2005. *Principles and Practice of Structural Equation Modelling*. Guilford Press, New York.
- Kumari, V., Ffytche, D.H., Williams, S.C., Gray, J.A., 2004. Personality predicts brain responses to cognitive demands. *J. Neurosci.* 24, 10636–10641.
- Matsumoto, K., Tanaka, K., 2004. Neuroscience. Conflict and cognitive control. *Science* 303, 969–970.
- Paus, T., 2001. Primate anterior cingulate cortex: where motor control, drive and cognition interface. *Nat. Rev., Neurosci.* 2, 417–424.
- Petroff, O.A., Errante, L.D., Kim, J.H., Spencer, D.D., 2003. *N*-acetyl-aspartate, total creatine, and myo-inositol in the epileptogenic human hippocampus. *Neurology* 60, 1646–1651.
- Picard, N., Strick, P.L., 2001. Imaging the premotor areas. *Curr. Opin. Neurobiol.* 11, 663–672.
- Provencher, S.W., 1993. Estimation of metabolite concentrations from localized in vivo proton NMR spectra. *Magn. Reson. Med.* 30, 672–679.
- Pujol, J., Lopez, A., Deus, J., Cardoner, N., Vallejo, J., Capdevila, A., Paus, T., 2002. Anatomical variability of the anterior cingulate gyrus and basic dimensions of human personality. *NeuroImage* 15, 847–855.
- Ridderinkhof, K.R., Ullsperger, M., Crone, E.A., Nieuwenhuis, S., 2004. The role of the medial frontal cortex in cognitive control. *Science* 306, 443–447.
- Ross, A.J., Sachdev, P.S., Wen, W., Valenzuela, M.J., Brodaty, H., 2005. Cognitive correlates of 1H MRS measures in the healthy elderly brain. *Brain Res. Bull.* 66, 9–16.
- Seminowicz, D.A., Mayberg, H.S., McIntosh, A.R., Goldapple, K., Kennedy, S., Segal, Z., Rafi-Tari, S., 2004. Limbic–frontal circuitry in major depression: a path modeling metanalysis. *NeuroImage* 22, 409–418.
- Smith, S.M., 2002. Fast robust automated brain extraction. *Hum. Brain Mapp.* 17, 143–155.
- Tabachnick, B.G., Fidell, L.S., 2001. *Using Multivariate Statistics*, 4th ed. Allyn and Bacon, New York.
- Torrubia, R., Avila, A., Molto, J., Caseras, X., 2001. The Sensitivity to Punishment and Sensitivity to Reward Questionnaire (SPSRQ) as a measure of Gray's anxiety and impulsivity dimensions. *Pers. Individ. Differ.* 31, 837–862.
- Valenzuela, M.J., Sachdev, P., 2001. Magnetic resonance spectroscopy in AD. *Neurology* 56, 592–598.
- Vogt, B.A., 2005. Pain and emotion interactions in subregions of the cingulate gyrus. *Nat. Rev., Neurosci.* 6, 533–544.
- Wechsler, D., 1999. *Wechsler Abbreviated Scale of Intelligence Manual*. The Psychological Corporation, San Antonio.
- Whittle, S., Allen, N.B., Lubman, D.I., Yücel, M., 2006. The neurobiological basis of temperament: towards a better understanding of psychopathology. *Neurosci. Biobehav. Rev.* 30, 511–525.
- Woolrich, M.W., Ripley, B.D., Brady, M., Smith, S.M., 2001. Temporal autocorrelation in univariate linear modeling of FMRI data. *NeuroImage* 14, 1370–1386.
- Woolrich, M.W., Behrens, T.E., Beckmann, C.F., Jenkinson, M., Smith, S.M., 2004. Multilevel linear modelling for FMRI group analysis using Bayesian inference. *NeuroImage* 21, 1732–1747.
- Worsley, K.J., Evans, A.C., Marrett, S., Neelin, P., 1992. A three-dimensional statistical analysis for CBF activation studies in human brain. *J. Cereb. Blood Flow Metab.* 12, 900–918.
- Yücel, M., Wood, S.J., Fornito, A., Riffkin, J., Velakoulis, D., Pantelis, C., 2003. Anterior cingulate dysfunction: implications for psychiatric disorders? *J. Psychiatry Neurosci.* 28, 350–354.